

Comment on “Prediction of lattice constant in cubic perovskites”

Roberto L. Moreira^{a,*}, Anderson Dias^b

^aDepartamento de Física, ICEx, UFMG, C.P. 702, Belo Horizonte-MG 30123-970, Brazil

^bDepartamento de Química, ICEB, UFOP, Ouro Preto-MG 35400-000, Brazil

Received 15 February 2007; received in revised form 27 March 2007; accepted 29 March 2007

Abstract

In a recent work by Jiang et al. [Prediction of lattice constant in cubic perovskites, *J. Phys. Chem. Solids* 67 (2006) 1531–1536], the interrelationship between lattice constant, ionic radii and tolerance factor of cubic perovskites has been established and an empirical equation was obtained. However, the assumption of incorrect ionic coordination led to an incorrect mathematical expression even though the average relative errors between predicted and observed lattice constants of 132 materials were below 1%. Here, corrected coefficients for that empirical expression are obtained, which would likely be useful for investigation of general perovskite materials.

© 2007 Elsevier Ltd. All rights reserved.

Keywords: A. Oxides; A. Inorganic compounds; A. Semiconductors; B. Epitaxial growth; B. Crystal growth

The prediction of lattice constant values for perovskite materials is of recognized importance, owing to the development of new materials designed for different applications, such as ferroelectric thin films, microwave and semiconductor technologies etc. [1–6]. Therefore, the methodology developed by Jiang et al. [1], which allows one to predict the lattice constants (a_{pred}) of cubic perovskites (ABX_3) by using the known ionic radii of the cations and anion, appears to be very useful and should likely become a key reference for materials scientists and engineers working in the field [7–10]. However, in their work, Jiang et al. used ionic radii of all ions A , B and X , for coordination numbers (CN) equal to 6, obtaining an incorrect expression for a_{pred} as a function of the ionic radii and tolerance factor. Once we truly believe on the importance of that procedure, the purpose of this work is to present the corrected coefficients for the Jiang's expression.

In perovskite structures, B cations are coordinated by six X anions, while A cations present CN = 12 (also coordinated by X anions). The X anions have CN = 2, being coordinated by two B cations, since the distance $A-O$ is

about 40% larger than the $B-O$ bond distance. The correct ionic radii (r_A , r_B , r_X), taken from Shannon's work [11] and other references [12–16] are presented in Table 1. Tolerance factors $\{t = (r_A + r_X)/[\sqrt{2}(r_B + r_X)]\}$ were recalculated and new coefficients (β , δ and γ) for Jiang's expression, $a_{\text{pred}} = 2\beta(r_B + r_X) + \gamma t - \delta$, were obtained. These coefficients are summarized in Tables 1 and 2, together with two sets of Jiang's coefficients and with the average relative errors for the 132 materials used for determining Jiang's expression. The second set (Jiang^b) was determined after using the correct β value obtained by those authors.

The difference in the empirical coefficients can be easily seen from the plots of lattice constant (a) versus $2(r_B + r_X)$, presented in Fig. 1, and $[2\beta(r_B + r_X) - a]$ versus the tolerance factor (t), Fig. 2, with the β values determined from the fits of Fig. 1. It can be seen that the correction of the ionic radii of A and X ions led to smaller $2(r_B + r_X)$ and larger t values, shifting the data in the figures and changing the fitting parameters. However, the linear trends in all cases are maintained, and the fits of the curves give $a = \alpha + 2\beta(r_B + r_X)$ in Fig. 1, and $2\beta(r_B + r_X) - a = -\gamma t + \delta$, in Fig. 2.

It is worthy noticing that an ideal cubic perovskite would have $t \approx 1$, while materials with smaller t values usually

*Corresponding author. Tel.: +55 31 3499 5624.

E-mail address: bmoreira@fisica.ufmg.br (R.L. Moreira).

Table 1
Ionic radii and lattice parameters for 132 perovskites (compound 57 is meaningless)

No.	Compound	a (Å)	r_A (Å)	r_B (Å)	r_X (Å)	t	$2(r_B + r_X)$	$2\beta(r_B + r_X) - a$	a_{pred} (Å)	Dev. (%)
1	CsIO ₃	4.674	1.88	0.95	1.35	0.993	4.60	-0.484	4.539	2.883
2	RbUO ₃	4.323	1.72	0.76	1.35	1.029	4.22	-0.479	4.234	2.064
3	KUO ₃	4.29	1.64	0.76	1.35	1.002	4.22	-0.446	4.203	2.021
4	RbPaO ₃	4.368	1.72	0.78	1.35	1.019	4.26	-0.488	4.259	2.490
5	KPaO ₃	4.341	1.64	0.78	1.35	0.993	4.26	-0.461	4.229	2.579
6	KTaO ₃	3.988	1.64	0.64	1.35	1.062	3.98	-0.363	4.053	1.638
7	BaFeO ₃	3.994	1.61	0.585	1.35	1.082	3.87	-0.469	3.975	0.476
8	BaMoO ₃	4.040	1.61	0.65	1.35	1.047	4.00	-0.396	4.053	0.333
9	BaNbO ₃	4.080	1.61	0.68	1.35	1.031	4.06	-0.382	4.091	0.259
10	BaSnO ₃	4.116	1.61	0.69	1.35	1.026	4.08	-0.400	4.103	0.315
11	BaHfO ₃	4.171	1.61	0.71	1.35	1.016	4.12	-0.418	4.128	1.027
12	BaZrO ₃	4.193	1.61	0.72	1.35	1.011	4.14	-0.422	4.141	1.245
13	BaIrO ₃	4.100	1.61	0.625	1.35	1.060	3.95	-0.502	4.023	1.879
14	EuTiO ₃	3.905	1.23	0.67	1.35	0.903	4.04	-0.225	3.927	0.565
15	NaWO ₃	3.850	1.39	0.62	1.35	0.983	3.94	-0.261	3.927	2.006
16	SnTaO ₃	3.880	1.10	0.68	1.35	0.853	4.06	-0.182	3.889	0.227
17	SrMnO ₃	3.806	1.44	0.53	1.35	1.049	3.76	-0.381	3.838	0.843
18	SrVO ₃	3.890	1.44	0.58	1.35	1.022	3.86	-0.374	3.898	0.214
19	SrFeO ₃	3.850	1.44	0.585	1.35	1.020	3.87	-0.325	3.904	1.415
20	SrTiO ₃	3.905	1.44	0.605	1.35	1.009	3.91	-0.343	3.929	0.615
21	SrTeO ₃	3.949	1.44	0.645	1.35	0.989	3.99	-0.315	3.979	0.757
22	SrMoO ₃	3.975	1.44	0.65	1.35	0.986	4.00	-0.331	3.985	0.257
23	SrNbO ₃	4.016	1.44	0.68	1.35	0.972	4.06	-0.318	4.023	0.182
24	SrSnO ₃	4.034	1.44	0.69	1.35	0.967	4.08	-0.318	4.036	0.052
25	SrHfO ₃	4.069	1.44	0.71	1.35	0.958	4.12	-0.316	4.062	0.175
26	CaVO ₃	3.767	1.34	0.58	1.35	0.986	3.86	-0.251	3.857	2.381
27	BaPbO ₃	4.265	1.61	0.775	1.35	0.985	4.25	-0.394	4.211	1.260
28	BaTbO ₃	4.285	1.61	0.76	1.35	0.992	4.22	-0.441	4.192	2.173
29	BaPrO ₃	4.354	1.61	0.85	1.35	0.951	4.40	-0.346	4.310	1.016
30	BaCeO ₃	4.397	1.61	0.87	1.35	0.943	4.44	-0.353	4.336	1.376
31	BaAmO ₃	4.357	1.61	0.85	1.35	0.951	4.40	-0.349	4.310	1.084
32	BaNpO ₃	4.384	1.61	0.87	1.35	0.943	4.44	-0.340	4.336	1.084
33	BaUO ₃	4.387	1.61	0.89	1.35	0.934	4.48	-0.306	4.363	0.539
34	BaPaO ₃	4.450	1.61	0.9	1.35	0.930	4.50	-0.351	4.377	1.644
35	BaThO ₃	4.480	1.61	0.94	1.35	0.914	4.58	-0.308	4.431	1.088
36	SrTbO ₃	4.180	1.44	0.76	1.35	0.935	4.22	-0.336	4.127	1.263
37	SrAmO ₃	4.230	1.44	0.85	1.35	0.897	4.40	-0.222	4.248	0.419
38	SrPuO ₃	4.280	1.44	0.86	1.35	0.893	4.42	-0.254	4.261	0.436
39	SrCoO ₃	3.850	1.44	0.53	1.35	1.049	3.76	-0.425	3.838	0.309
40	BaTiO ₃	4.012	1.61	0.605	1.35	1.071	3.91	-0.450	3.999	0.328
41	CaTiO ₃	3.840	1.34	0.605	1.35	0.973	3.91	-0.278	3.888	1.248
42	CeAlO ₃	3.772	1.34	0.535	1.35	1.009	3.77	-0.338	3.801	0.781
43	EuAlO ₃	3.725	1.23	0.535	1.35	0.968	3.77	-0.291	3.755	0.794
44	EuCrO ₃	3.803	1.23	0.615	1.35	0.928	3.93	-0.223	3.856	1.383
45	EuFeO ₃	3.836	1.23	0.645	1.35	0.914	3.99	-0.206	3.894	1.522
46	GdAlO ₃	3.710	1.22	0.535	1.35	0.964	3.77	-0.276	3.750	1.087
47	GdCrO ₃	3.795	1.22	0.615	1.35	0.925	3.93	-0.215	3.852	1.489

48	GdFeO ₃	3.820	1.22	0.645	1.35	0.911	3.99	-0.186	3.890	1.842
49	KNbO ₃	4.007	1.64	0.64	1.35	1.062	3.98	-0.382	4.053	1.156
50	LaAlO ₃	3.778	1.36	0.535	1.35	1.017	3.77	-0.344	3.810	0.846
51	LaCrO ₃	3.874	1.36	0.615	1.35	0.975	3.93	-0.294	3.909	0.896
52	LaFeO ₃	3.920	1.36	0.645	1.35	0.961	3.99	-0.286	3.947	0.681
53	LaGaO ₃	3.874	1.36	0.62	1.35	0.973	3.94	-0.285	3.915	1.058
54	LaRhO ₃	3.940	1.36	0.665	1.35	0.951	4.03	-0.269	3.972	0.820
55	LaTiO ₃	3.920	1.36	0.67	1.35	0.949	4.04	-0.240	3.979	1.499
56	LaVO ₃	3.910	1.36	0.64	1.35	0.963	3.98	-0.285	3.940	0.776
57	NaAlO ₃	3.730	1.39	0.535	1.35	1.028	3.77	-0.296	3.823	2.486
58	NaTaO ₃	3.881	1.39	0.64	1.35	0.974	3.98	-0.256	3.952	1.841
59	NdAlO ₃	3.752	1.27	0.535	1.35	0.983	3.77	-0.320	3.772	0.523
60	NdCoO ₃	3.777	1.27	0.545	1.35	0.978	3.79	-0.325	3.784	0.184
61	NdCrO ₃	3.835	1.27	0.615	1.35	0.943	3.93	-0.255	3.872	0.963
62	NdFeO ₃	3.870	1.27	0.645	1.35	0.929	3.99	-0.236	3.910	1.046
63	NdMnO ₃	3.800	1.27	0.645	1.35	0.929	3.99	-0.166	3.910	2.907
64	PrAlO ₃	3.757	1.30	0.535	1.35	0.994	3.77	-0.323	3.784	0.729
65	PrCrO ₃	3.852	1.30	0.615	1.35	0.954	3.93	-0.272	3.884	0.835
66	PrFeO ₃	3.887	1.30	0.645	1.35	0.939	3.99	-0.253	3.923	0.915
67	PrGaO ₃	3.863	1.30	0.62	1.35	0.951	3.94	-0.274	3.891	0.713
68	PrMnO ₃	3.820	1.30	0.645	1.35	0.939	3.99	-0.186	3.923	2.685
69	PrVO ₃	3.890	1.30	0.64	1.35	0.942	3.98	-0.265	3.916	0.672
70	SmAlO ₃	3.734	1.24	0.535	1.35	0.972	3.77	-0.300	3.759	0.665
71	SmCoO ₃	3.750	1.24	0.545	1.35	0.966	3.79	-0.298	3.771	0.567
72	SmVO ₃	3.890	1.24	0.64	1.35	0.920	3.98	-0.265	3.892	0.049
73	SmFeO ₃	3.845	1.24	0.645	1.35	0.918	3.99	-0.211	3.898	1.389
74	SrZrO ₃	4.101	1.44	0.72	1.35	0.953	4.14	-0.330	4.075	0.638
75	YAlO ₃	3.680	1.20	0.535	1.35	0.957	3.77	-0.246	3.742	1.679
76	YCrO ₃	3.768	1.20	0.615	1.35	0.918	3.93	-0.188	3.843	1.999
77	YFeO ₃	3.785	1.20	0.645	1.35	0.904	3.99	-0.151	3.882	2.570
78	CsCdF ₃	4.470	1.88	0.95	1.285	1.001	4.47	-0.398	4.430	0.888
79	CsCaF ₃	4.523	1.88	1.00	1.285	0.979	4.57	-0.360	4.496	0.586
80	CsHgF ₃	4.570	1.88	1.02	1.285	0.971	4.61	-0.371	4.523	1.023
81	CsSrF ₃	4.750	1.88	1.18	1.285	0.908	4.93	-0.259	4.743	0.147
82	TiCoF ₃	4.138	1.70	0.745	1.285	1.040	4.06	-0.440	4.100	0.907
83	TiFeF ₃	4.188	1.70	0.78	1.285	1.022	4.13	-0.426	4.144	1.046
84	TiMnF ₃	4.260	1.70	0.83	1.285	0.998	4.23	-0.407	4.208	1.224
85	TiCdF ₃	4.400	1.70	0.95	1.285	0.944	4.47	-0.328	4.366	0.782
86	NH ₄ ZnF ₃	4.115	1.80	0.74	1.285	1.077	4.05	-0.426	4.134	0.459
87	NH ₄ CoF ₃	4.129	1.80	0.745	1.285	1.075	4.06	-0.431	4.140	0.266
88	NH ₄ FeF ₃	4.177	1.80	0.78	1.285	1.056	4.13	-0.415	4.183	0.145
89	NH ₄ MnF ₃	4.241	1.80	0.83	1.285	1.031	4.23	-0.388	4.246	0.113
90	RbZnF ₃	4.122	1.72	0.74	1.285	1.049	4.05	-0.433	4.102	0.481
91	RbCoF ₃	4.141	1.72	0.745	1.285	1.047	4.06	-0.443	4.108	0.788
92	RbVF ₃	4.170	1.72	0.79	1.285	1.024	4.15	-0.390	4.165	0.131
93	RbFeF ₃	4.174	1.72	0.78	1.285	1.029	4.13	-0.412	4.152	0.528
94	RbMnF ₃	4.240	1.72	0.83	1.285	1.005	4.23	-0.387	4.215	0.579
95	RbCdF ₃	4.398	1.72	0.95	1.285	0.951	4.47	-0.326	4.373	0.573
96	RbCaF ₃	4.452	1.72	1.00	1.285	0.930	4.57	-0.289	4.440	0.264
97	RbHgF ₃	4.470	1.72	1.02	1.285	0.922	4.61	-0.271	4.468	0.055
98	KCdF ₃	4.293	1.64	0.95	1.285	0.925	4.47	-0.221	4.344	1.189
99	KMgF ₃	3.989	1.64	0.72	1.285	1.032	4.01	-0.336	4.046	1.419

Table 1 (continued)

No.	Compound	a (Å)	r_A (Å)	r_B (Å)	r_X (Å)	t	$2(r_B + r_X)$	$2\beta(r_B + r_X) - a$	a_{pred} (Å)	Dev. (%)
100	KNiF ₃	4.013	1.64	0.69	1.285	1.047	3.95	-0.415	4.009	0.106
101	KZnF ₃	4.056	1.64	0.74	1.285	1.021	4.05	-0.367	4.070	0.356
102	KCoF ₃	4.071	1.64	0.745	1.285	1.019	4.06	-0.373	4.077	0.140
103	KVF ₃	4.100	1.64	0.79	1.285	0.997	4.15	-0.320	4.134	0.819
104	KFeF ₃	4.121	1.64	0.78	1.285	1.002	4.13	-0.359	4.121	0.003
105	KMnF ₃	4.189	1.64	0.83	1.285	0.978	4.23	-0.336	4.185	0.094
106	AgMgF ₃	3.918	1.48	0.72	1.285	0.975	4.01	-0.265	3.982	1.621
107	AgNiF ₃	3.936	1.48	0.69	1.285	0.990	3.95	-0.338	3.944	0.195
108	AgZnF ₃	3.972	1.48	0.74	1.285	0.966	4.05	-0.283	4.007	0.881
109	AgCoF ₃	3.983	1.48	0.745	1.285	0.963	4.06	-0.285	4.013	0.764
110	AgMnF ₃	4.030	1.48	0.83	1.285	0.924	4.23	-0.177	4.124	2.340
111	NaVF ₃	3.940	1.39	0.79	1.285	0.912	4.15	-0.160	4.037	2.458
112	RbPdF ₃	4.298	1.72	0.86	1.285	0.991	4.29	-0.390	4.254	1.021
113	NH ₄ MgF ₃	4.060	1.80	0.72	1.285	1.088	4.01	-0.407	4.110	1.223
114	TlPdF ₃	4.301	1.70	0.86	1.285	0.984	4.29	-0.393	4.247	1.264
115	LiBaF ₃	3.992	1.61	0.76	1.285	1.001	4.09	-0.267	4.084	2.299
116	RbYbF ₃	4.530	1.72	1.02	1.285	0.922	4.61	-0.331	4.468	1.379
117	CsEuF ₃	4.780	1.88	1.17	1.285	0.912	4.91	-0.308	4.729	1.064
118	CsPbF ₃	4.800	1.88	1.19	1.285	0.904	4.95	-0.291	4.757	0.891
119	CsYbF ₃	4.610	1.88	1.02	1.285	0.971	4.61	-0.411	4.523	1.882
120	RbPbF ₃	4.790	1.72	1.19	1.285	0.859	4.95	-0.281	4.705	1.768
121	CsCaCl ₃	5.396	1.88	1.00	1.79	0.930	5.58	-0.313	5.360	0.658
122	CsCdCl ₃	5.210	1.88	0.95	1.79	0.947	5.48	-0.218	5.289	1.510
123	CsPbCl ₃	5.605	1.88	1.19	1.79	0.871	5.96	-0.176	5.639	0.612
124	CsHgCl ₃	5.410	1.88	1.02	1.79	0.924	5.62	-0.291	5.389	0.381
125	TlMnCl ₃	5.020	1.70	0.83	1.79	0.942	5.24	-0.247	5.064	0.880
126	CsEuCl ₃	5.627	1.88	1.17	1.79	0.877	5.92	-0.235	5.610	0.311
127	CsTmCl ₃	5.476	1.88	1.03	1.79	0.920	5.64	-0.339	5.404	1.317
128	CsYbCl ₃	5.437	1.88	1.02	1.79	0.924	5.62	-0.318	5.389	0.875
129	CsHgBr ₃	5.770	1.88	1.02	1.95	0.912	5.94	-0.359	5.668	1.774
130	CsPbBr ₃	5.874	1.88	1.19	1.95	0.862	6.28	-0.154	5.921	0.805
131	CsSnBr ₃	5.795	1.88	0.95	1.95	0.934	5.80	-0.512	5.565	3.967
132	CsSnI ₃	6.219	1.88	0.95	2.16	0.919	6.22	-0.553	5.930	4.642
								Average deviation (%)		1.07

Ionic radii for Cl, Br, I, Ag, Sn, and lanthanides from Refs. [12–16].

Table 2

Empirical coefficients for determining the lattice constants of cubic perovskites, with the expression $a_{\text{pred}} = 2\beta(r_B + r_X) + \gamma t - \delta$

	β	γ	δ	% error
Jiang ^a	0.9418	1.4898	1.2062	0.63
Jiang ^b	0.9148	1.4314	1.0368	0.63
This work	0.9109	1.1359	0.7785	1.07

Jiang^a are the coefficients given in Ref. [1] with incorrect β value; Jiang^b are the coefficients with correct β value for the same work.

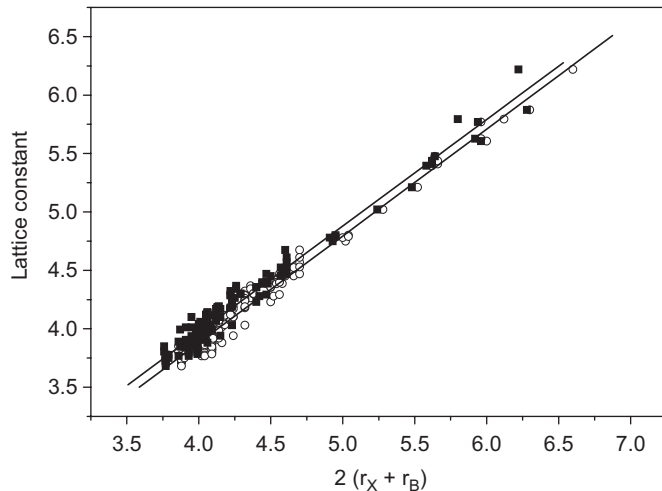


Fig. 1. Linear fits used for determining the β parameter. Here, $a = \alpha + 2\beta(r_B + r_X)$. Open circles for data of Ref. [1]; full squares are our corrected data. Both axes in Angstroms.

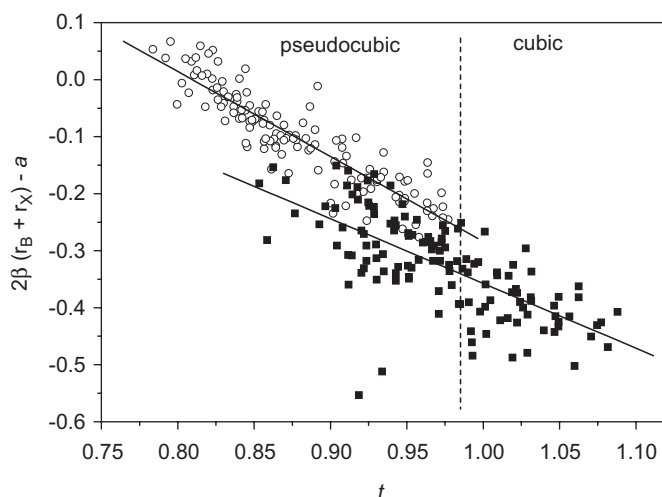


Fig. 2. Linear fits of $2\beta(r_B + r_X) - a = -\gamma t + \delta$, for obtaining the parameters γ and δ . Same symbols as in Fig. 1. The dashed line indicates the critical line for cubic structures. Vertical axis in Angstroms.

belong to lower symmetry structures, with tilted BX_6 octahedra [17]. The critical t value for stabilizing cubic structures is about 0.985 [17]. This value is higher than those obtained in Ref. [1] for all the 132 materials investigated. Take for instance SrTiO_3 : according to Ref. [1],

this material would present $t = 0.908$, indicating that it would belong to a distorted/tilted non-cubic structure; after the correction proposed here, t becomes 1.009, in agreement with its experimentally observed untilted cubic structure (at room temperature) [18]. Another remark concerns the increase in the average deviation between predicted and experimental lattice parameters. As it can be seen in Fig. 2, the dispersion of data increased after correction of the CN's. This could be due to a lower accuracy of ionic radii used for CN = 12 (worse statistics than for CN = 6), although we should remember that most structures are indeed pseudocubic, with tilted BX_6 octahedra, which change both, the approximated a value (i.e., the cubic ratio of the unit cell volume) as well as the “average” ionic radii used in the calculations.

In conclusion, we believe that the empirical expression for determining the lattice parameters of cubic perovskites developed in Ref. [1], with the corrections presented here, could be very useful in future researches in this field.

Acknowledgements

This work was partially supported by the Brazilian agencies MCT/CNPq, FINEP and FAPEMIG.

References

- [1] L.Q. Jiang, J.K. Guo, H.B. Lin, M. Zhu, X. Zhou, P. Wu, C.H. Li, Prediction of lattice constant in cubic perovskites, *J. Phys. Chem. Solids* 67 (2006) 1531–1536.
- [2] R. Ramesh, N.A. Spaldin, Multiferroics: progress and prospects in thin films, *Nature Mater.* 6 (2007) 21–29.
- [3] J.F. Scott, Nanoferroelectrics: statics and dynamics, *J. Phys. Condens. Mater.* 18 (2006) R361–R386.
- [4] A.A. Bokov, Z.G. Ye, Recent progress in relaxor ferroelectrics with perovskite structure, *J. Mater. Sci.* 41 (2006) 31–52.
- [5] R.M. Ormerod, Solid oxide fuel cells, *Chem. Soc. Rev.* 32 (2003) 17–28.
- [6] P. Knauth, H.L. Tuller, Solid-state ionics: root, status and future prospects, *J. Am. Ceram. Soc.* 85 (2002) 1654–1680.
- [7] A.S. Bhalla, R.Y. Guo, R. Roy, The perovskite structure—a review of its role in ceramic science and technology, *Mater. Res. Innov.* 4 (2000) 3–26.
- [8] E.Y. Tsybal, H. Kohlstedt, Applied physics—tunneling across a ferroelectric, *Science* 313 (2006) 181–183.
- [9] Y.H. Huang, R.I. Dass, Z.L. Xing, J.B. Goodenough, Double perovskites as anode materials for solid-oxide fuel cells, *Science* 312 (2006) 254–257.
- [10] H. Yamada, Y. Ogawa, Y. Ishii, H. Sato, M. Kawasaki, H. Akoh, Y. Rokura, Engineered interface of magnetic oxides, *Science* 305 (2004) 646–648.
- [11] R.D. Shannon, Revised effective ionic radii and systematic studies of interatomic distances in halides and chalcogenides, *Acta Cryst. A* 32 (1976) 751–767.
- [12] K. Makino, K. Tomita, K. Suwa, Effect of chlorine on the crystal-structure of a chlorine-rich hastingsite, *Miner. Mag.* 57 (1993) 677–685.
- [13] T. Li, G.D. Stucky, G.L. McPherson, *Acta Cryst. B* 29 (1973) 1330–1335.

- [14] L.A. Groat, J.L. Jambor, B.C. Pemberton, The crystal structure of argentojarosite, $\text{AgFe}_3(\text{SO})_4(\text{OH})_6$, *Can. Miner.* 41 (2003) 921–928.
- [15] R.A. Howie, W. Moser, I.C. Trevena, The crystal structure of tin(II) iodide, *Acta Cryst. B* 28 (1972) 2965–2971.
- [16] Y. Tomioka, Y. Okimoto, J.H. Jung, R. Kumai, Y. Tokura, Phase diagrams of perovskite-type manganese oxides, *J. Phys. Chem. Solids* 67 (2006) 2214–2221.
- [17] I.M. Reaney, D. Iddles, Microwave dielectric ceramics for resonators and filters in mobile phone networks, *J. Am. Ceram. Soc.* 89 (2006) 2063–2072.
- [18] T. Hirata, K. Ishioka, M. Kitajima, Vibrational spectroscopy and X-ray diffraction of perovskite compounds $\text{Sr}_{1-x}\text{M}_x\text{TiO}_3$ ($\text{M} = \text{Ca}, \text{Mg}; 0 \leq x \leq 1$), *J. Solid State Chem.* 124 (1996) 353–359.